Rac1 GTPase regulates 11β hydroxysteroid dehydrogenase type 2 and fibrotic remodeling

Received for publication, October 23, 2016, and in revised form, March 9, 2017 Published, Papers in Press, March 20, 2017, DOI 10.1074/jbc.M116.764449

Daniel Lavall[1], **Pia Schuster, Nadine Jacobs, Andrey Kazakov, Michael Böhm, and Ulrich Laufs**

From the Universität des Saarlandes, Klinik für Innere Medizin III—Kardiologie, Angiologie und Internistische Intensivmedizin, Universitätsklinikum des Saarlandes, D-66421 Homburg/Saar, Germany

Edited by Henrik G. Dohlman

The aim of the study was to characterize the role of Rac1 GTPase for the mineralocorticoid receptor (MR)-mediated pro-fibrotic remodeling. Transgenic mice with cardiac overexpression of constitutively active Rac1 (RacET) develop an age-dependent phenotype with atrial dilatation, fibrosis, and atrial fibrillation. Expression of MR was similar in RacET and WT mice. The expression of 11β hydroxysteroid dehydrogenase type 2 (11β-HSD2) was age-dependently up-regulated in the atria and the left ventricles of RacET mice on mRNA and protein levels. Statin treatment inhibiting Rac1 geranylgeranylation reduced 11β-HSD2 up-regulation. Samples of human left atrial myocardium showed a positive correlation between Rac1 activity and 11β-HSD2 expression ($r = 0.7169$). Immunoprecipitation showed enhanced Rac1-bound 11β-HSD2 relative to Rac1 expression in RacET mice that was diminished with statin treatment. Both basal and phorbol 12-myristate 13-acetate (PMA)-induced NADPH oxidase activity were increased in RacET and correlated positively with 11β-HSD2 expression ($r = 0.788$ and $r = 0.843$, respectively). In cultured H9c2 cardiomyocytes, Rac1 activation with L-buthionine sulfoximine increased; Rac1 inhibition with NSC23766 decreased 11β-HSD2 mRNA and protein expression. Connective tissue growth factor (CTGF) up-regulation induced by aldosterone was prevented with NSC23766. Cardiomyocyte transfection with 11β-HSD2 siRNA abolished the aldosterone-induced CTGF up-regulation. Aldosterone-stimulated MR nuclear translocation was blocked by the 11β-HSD2 inhibitor carbenoxolone. In cardiac fibroblasts, nuclear MR translocation induced by aldosterone was inhibited with NSC23766 and spironolactone. NSC23766 prevented the aldosterone-induced proliferation and migration of cardiac fibroblasts and the up-regulation of CTGF and fibronectin. In conclusion, Rac1 GTPase regulates 11β-HSD2 expression, MR activation, and MR-mediated pro-fibrotic signaling.

Cardiac fibrosis is the hallmark of structural remodeling and occurs under several pathophysiological conditions such as arterial hypertension and aortic stenosis and after myocardial infarction (1). Left ventricular fibrosis is a strong risk factor for the development of arrhythmias and heart failure (2). Atrial fibrosis predisposes for atrial fibrillation (3), the most common arrhythmia (4).

Activation of the mineralocorticoid receptor (MR)[2] induces cardiac fibrosis both *in vitro* and *in vivo* (5). MR antagonists such as spironolactone and eplerenone are able to prevent cardiac fibrosis (6). Furthermore, MR antagonists are a mainstay in the medical therapy of chronic heart failure because they improve survival (7). However, the molecular mechanisms of MR-mediated structural cardiac remodeling that underlie these clinical benefits are poorly understood.

We have previously identified MR downstream pathways leading to cardiac fibrosis in atrial fibrillation (8). Atrial fibrillation is also associated with Rac1 activation, which in turn induces atrial fibrosis (9, 10). Therefore, we hypothesized that there may be a functional interaction between Rac1 and the MR relevant for the molecular pathways leading to cardiac fibrosis.

Results

The Rac1-dependent phenotype with atrial fibrillation, dilatation, and fibrosis

Transgenic mice with the heart-specific overexpression of constitutively active V12Rac1 (RacET) mice develop age-dependent atrial dilatation and increased left atrial (LA) weight relative to tibia length WT control, 0.30 ± 0.05 mg/mm, *versus* RacET 12, 0.43 ± 0.05 mg/mm, $p = 0.048$) (Fig. 1*A*) and to the weight of the left ventricle (LV) (WT, 5.4 ± 1.1%, *versus* RacET 12, 8.3 ± 1.8%, $p = 0.02$) (Fig. 1*B*). Left atrial structural remodeling in 12-month-old RacET mice is characterized by elevated connective tissue growth factor (CTGF) gene (149 ± 39%, $p = 0.033$, *versus* WT) (Fig. 1*C*) and protein (142 ± 13%, $p = 0.003$, *versus* WT) (Fig. 1*D*) expression. Lysyl oxidase (LOX) expression was increased (186 ± 32%, $p = 0.0009$, *versus* WT) (Fig. 1*E*) and Sprouty-1, the downstream target of microRNA-21, decreased (54 ± 12%, $p = 0.036$, *versus* WT) (Fig. 1*F*) in RacET mice. RacET mice develop age-dependent atrial fibrillation and atrial flutter (43% in RacET 6, 77% RacET 12) (Fig. 1*G*). In the left atrium, collagen content at 12 months was increased (Fig. 1*H*).

This work was supported by the Universität des Saarlandes and by the Deutsche Forschungsgemeinschaft (DFG KA 4024/3-1). The authors declare that they have no conflicts of interest with the contents of this article.

[1] To whom correspondence should be addressed: Kirrberger Strasse, D-66421 Homburg/Saar, Germany. Tel.: 49-6841-16-15000; E-mail: daniel.lavall@uks.eu.

[2] The abbreviations used are: MR, mineralocorticoid receptor; 11β-HSD2, 11β hydroxysteroid dehydrogenase type 2; BSO, L-buthionine sulfoximine; CTGF, connective tissue growth factor; LOX, lysyl oxidase; PMA, phorbol 12-myristate 13-acetate; RacET, transgenic mice with cardiac overexpression of constitutive active Rac1; TRITC, tetramethylrhodamine isothiocyanate; DAPI, 4′, 6′ diamidino-2-phenylindole.

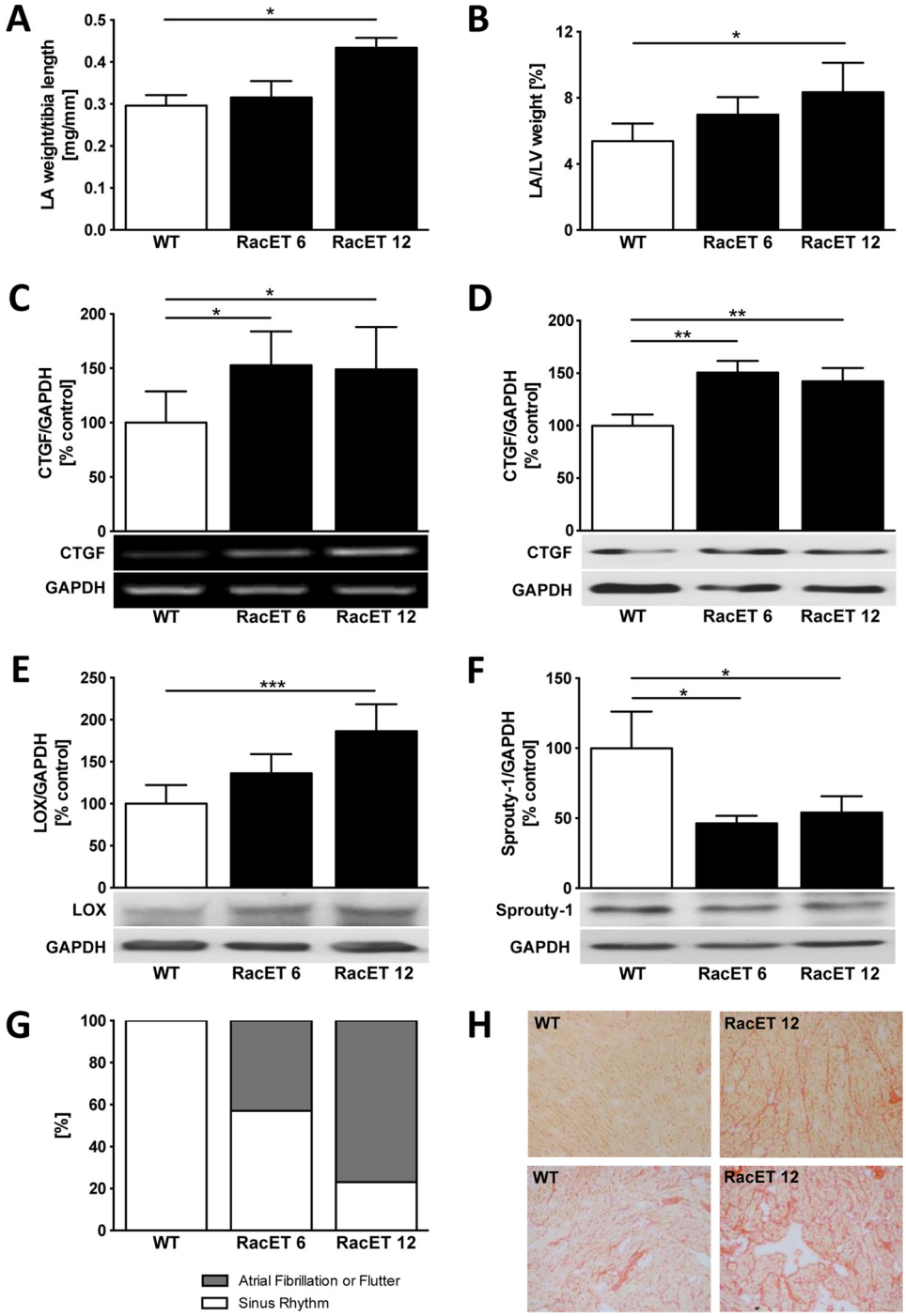

Figure 1. The RacET phenotype with age-dependent atrial dilatation, fibrosis, and atrial fibrillation. *A* and *B*, left atrial (*LA*) weight relative to tibia length (*A*) and to left ventricular (*LV*) weight (*B*) in transgenic mice with heart-specific overexpression of Rac1 at 6 (*RacET 6*) and 12 (*RacET 12*) months of age compared with WT control mice (FVBN). *C* and *D*, quantification of connective tissue growth factor (*CTGF*) mRNA (*C*, RT-PCR) and protein (*D*, Western blot) expression in LA of RacET mice. GAPDH was used as loading control. *E* and *F*, lysyl oxidase (*E*, *LOX*) and Sprouty-1 (*F*) myocardial protein expression in the RacET 6 and 12 months compared with WT mice. *G*, prevalence of atrial fibrillation and flutter evaluated by electrocardiography. *H*, Sirius red staining of left atrial myocardium of WT and 12-month-old RacET mice in ×10 (*upper panel*) and ×100 (*lower panel*) magnification. *Error bars* indicate means ± S.D. *, $p < 0.05$; **, $p < 0.01$; ***, $p < 0.001$.

Increased expression of 11β-HSD2 in RacET mice

The atrial protein expression of the mineralocorticoid receptor (MR) was unchanged in RacET mice (Fig. 2*A*) compared with WT control mice. The expression of 11β-HSD2, the enzyme that inactivates cortisol providing aldosterone access to the MR, increased with age in the atria of RacET (RacET 12, 665 ± 378%, $p = 0.043$, *versus* WT) (Fig. 2*B*). Similar changes were found in the left ventricle of RacET mice for the expression of MR (Fig. 2*C*) and 11β-HSD2 (RacET 12, 452 ± 415%, $p = 0.040$, *versus* WT) (Fig. 2*D*). Expression of 11β-HSD2 mRNA was similar on both atrial (RacET 12, 401 ± 482%, $p = 0.033$, *versus* WT) (Fig. 2*E*) and ventricular (RacET 12, 1113 ± 840%, $p = 0.004$, *versus* WT) (Fig. 2*F*) levels. Treatment of RacET mice with rosuvastatin inhibiting Rac1 GTPase by

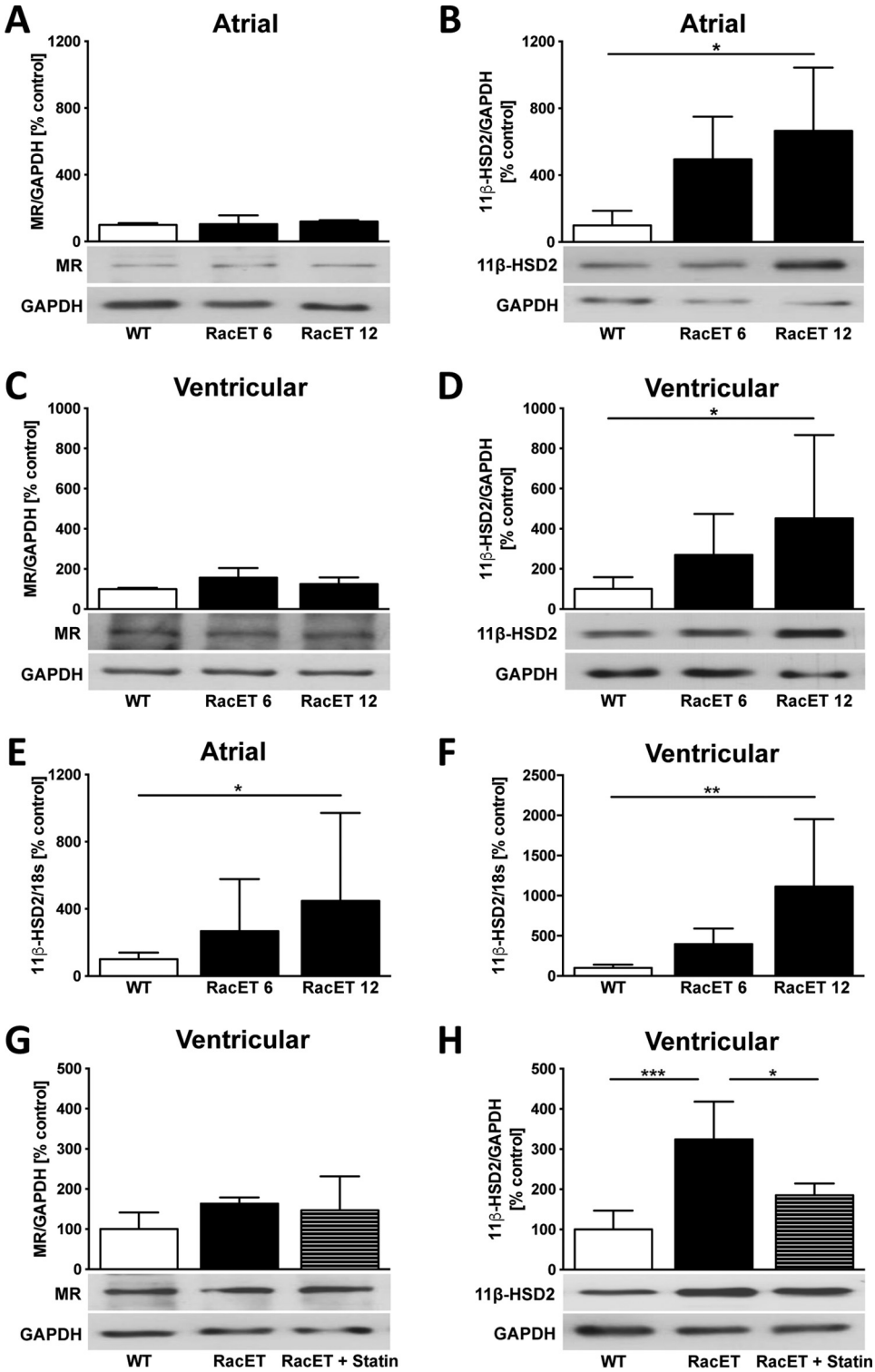

Figure 2. Increased expression of 11β-HSD2 in RacET mice. *A* and *B*, Western blotting analysis showing atrial protein expression (Western blot) of the mineralocorticoid receptor (*MR*) (*A*) and 11β hydroxysteroid dehydrogenase type 2 (*11β-HSD2*) (*B*) in 6-month-old (*RacET 6*) and 12-month-old (*RacET 12*) RacET compared with WT control mice. *C* and *D*, ventricular MR and 11β-HSD2 protein expression in 6- and 12-month-old RacET mice compared with WT mice. *E* and *F*, atrial (*E*) and ventricular (*F*) mRNA expression (TaqMan gene expression assay) of 11β-HSD2 in RacET 6 and RacET 12 compared with WT control. *G* and *H*, MR (*G*) and 11β-HSD2 (*H*) protein expression in RacET mice treated with 0.4 mg/day rosuvastatin (*RacET + statin*) or vehicle (*RacET*) for 10 months compared with WT mice. *Error bars* indicate means ± S.D. *, $p < 0.05$; **, $p < 0.01$; ***, $p < 0.001$.

blocking its posttranslational geranylgeranylation (11) over 10 months did not alter MR expression (Fig. 2*G*) but reduced the 11β-HSD2 up-regulation in the left ventricle compared with vehicle-treated RacET mice (RacET, 324 ± 94%, $p = 0.0005$, *versus* WT; RacET + statin, 185 ± 29%, $p = 0.015$, *versus* RacET) (Fig. 2*H*).

Young (*i.e.* 2 months old) RacET mice had similar atrial dimensions, no signs of cardiac fibrosis, and similar CTGF

expression compared with wild type control mice. Also, these RacET mice showed both unaltered 11β-HSD2 expression and NADPH oxidase activity compared with WT mice (data not shown).

Interaction of Rac1 and 11β-HSD2

We have observed previously that left atrial myocardium from patients with atrial fibrillation who underwent mitral valve cardiac surgery is characterized by both increased Rac1 activity (10) and 11β-HSD2 expression (8) compared with patients in sinus rhythm. In the left atrial myocardium of these patients there was a positive correlation between the Rac1 activity and the 11β-HSD2 expression ($r = 0.717$, $p = 0.037$) (Fig. 3*A*). In RacET mice, Rac1-bound 11β-HSD2 relative to Rac1 protein expression was elevated (271 ± 79%, $p = 0.011$, *versus* WT) (Fig. 3*B*). Statin-treated RacET mice showed an intermediate amount of Rac1-bound 11β-HSD2 between WT and vehicle-treated RacET mice. Immunohistochemical staining demonstrated an accumulation of 11β-HSD2 at the side of cardiomyocyte cell membranes and in capillaries. In WT mice, 11β-HSD2 was not detectable by immunostaining (Fig. 3*C*). In statin-treated RacET, 11β-HSD2-positive staining was markedly reduced. RacET mice are characterized by increased NADPH oxidase activity both basal and phorbol-12-myristate13-acetate (PMA)-induced (184 ± 19%, $p = 0.046$, *versus* WT and 286 ± 127%, $p = 0.0002$, *versus* WT, respectively) (Fig. 3*D*). PMA is a nonspecific stimulator of NADPH oxidase. Statin treatment reduced these effects on NADPH oxidase activity (123 ± 35%, $p = 0.0008$, *versus* RacET). Both basal and PMA-induced NADPH oxidase activity correlated positively with 11β-HSD2 protein expression in these mice ($r = 0.788$, $p = 0.020$ and $r = 0.843$, $p = 0.017$, respectively) (Fig. 3, *E* and *F*). Treatment of cultured cardiomyocytes with L-buthionine sulfoximine (BSO), a redox-dependent Rac1 activator generating reactive oxygen species (12), increased 11β-HSD2 expression on both protein and mRNA levels (174 ± 47%, $p = 0.010$ and 155 ± 15%, $p = 0.0002$, respectively) (Fig. 3, *G* and *I*). Conversely, 11β-HSD2 protein and mRNA expression decreased after treatment with NSC23766, a specific Rac1 inhibitor (21 ± 7%, $p = 0.023$ and 73 ± 8%, $p = 0.011$, respectively) (Fig. 3, *H* and *I*).

Rac1 and 11β-HSD2 control the aldosterone-induced CTGF up-regulation

Aldosterone increased CTGF protein expression time dependently in cardiomyocytes; the effect was most pronounced after 48 h of treatment (24 h, 207 ± 45%, $p = 0.032$, *versus* control; 48 h, 268 ± 66%, $p = 0.001$, *versus* control) (Fig. 4*A*). Rac1 activation with BSO treatment elevated CTGF expression (152 ± 37%, $p = 0.004$, *versus* control) (Fig. 4*B*). The aldosterone-induced CTGF overexpression was completely prevented by preincubation with the Rac1 inhibitor NSC23766 (aldosterone + NSC23766, 77 ± 6%, $p = 0.003$, *versus* aldosterone) (Fig. 4*C*). Specific 11β-HSD2 silencing with siRNA transfection abolished the aldosterone effect on CTGF overexpression (aldosterone, 181 ± 35%, $p = 0.0095$, *versus* control; aldosterone + 11β-HSD2 siRNA, 123 ± 9%, $p = 0.047$, *versus* aldosterone) (Fig. 4*D*) in cardiomyocytes.

Inhibition of 11β-HSD2 suppressed the aldosterone-induced MR nuclear translocation

Carbenoxolone, an 11β-HSD2 inhibitor (13), dose-dependently decreased 11β-HSD2 protein expression in cardiomyocytes (carbenoxolone 100 μM, 44 ± 19%, $p = 0.019$, *versus* control) (Fig. 5*A*). Carbenoxolone prevented the aldosterone-induced nuclear translocation of the MR (aldosterone, 213 ± 70%, *versus* aldosterone + carbenoxolone 100 μM, 46 ± 45%, $p = 0.001$) (Fig. 5, *B* and *C*).

In cardiac fibroblasts, Rac1 regulates MR nuclear translocation, proliferation, and pro-fibrotic mediators

Aldosterone induced nuclear translocation of the mineralocorticoid receptor in cardiac fibroblasts (control, 0.07 ± 0.07, *versus* aldosterone, 0.84 ± 0.69, $p < 0.0001$) that was prevented by the MR antagonist spironolactone (0.25 ± 0.3, $p = 0.0009$, *versus* aldosterone) and the Rac1 inhibitor NSC23766 (0.21 ± 0.17, $p = 0.0003$, *versus* aldosterone) (Fig. 6, *A* and *B*). Aldosterone induced cardiac fibroblast proliferation (161 ± 31%, $p < 0.0001$) (Fig. 6*C*) and migration (117 ± 16%, $p = 0.035$) (Fig. 6*D*) that were both prevented by NCS23766 (59 ± 26%, $p < 0.0001$, *versus* aldosterone, and 94 ± 11%, $p = 0.002$, *versus* aldosterone, respectively). Aldosterone up-regulates CTGF (182 ± 55%, $p = 0.031$, *versus* control), whereas NSC23766 pretreatment decreased CTGF expression (39 ± 5%, $p = 0.003$, *versus* aldosterone) (Fig. 6*E*). CTGF treatment in cardiac fibroblasts dose-dependently induced fibronectin (CTGF 1 ng/ml, 277 ± 33%, $p = 0.022$, *versus* control; CTGF 10 ng/ml, 368 ± 111%, $p = 0.002$, *versus* control) (Fig. 6*F*). Furthermore, fibronectin was up-regulated by aldosterone (181 ± 43%, $p = 0.013$, *versus* control) via a Rac1-dependent pathway because NSC23766 prevented the aldosterone-induced up-regulation (aldosterone + NSC23766, 94 ± 27%, $p = 0.035$, *versus* aldosterone) (Fig. 6*G*).

Discussion

This study in transgenic RacET mice, cultured cardiac myocytes and fibroblasts, and human left atrial myocardium shows that Rac1 regulates 11β hydroxysteroid dehydrogenase type 2. These changes are age-dependently associated with structural atrial remodeling and arrhythmias. In cardiomyocytes, the Rac1-mediated increase of 11β-HSD2 facilitated the aldosterone-driven MR nuclear translocation and up-regulation of the pro-fibrotic mediator CTGF. Rac1 inhibition prevented nuclear translocation, proliferation, and migration, as well as CTGF and fibronectin overexpression in cardiac fibroblasts.

Mice with cardiac-specific overexpression of constitutively active Rac1 (RacET) develop atrial fibrillation with increasing age (10). This study characterizes the age-dependent structural remodeling consisting of atrial enlargement; CTGF, LOX, and Sprouty-1 overexpression; and collagen deposition that predisposes for atrial arrhythmias. Despite the limitations of any transgenic mice model, this distinct phenotype with atrial dilatation, fibrosis, and atrial fibrillation uniquely parallels the pathophysiology of atrial fibrillation in humans (3). Therefore, the RacET mice model is helpful for the study of structural changes during or preceding atrial fibrillation. Our study demonstrates an up-regulation of 11β-HSD2 in RacET mice as well

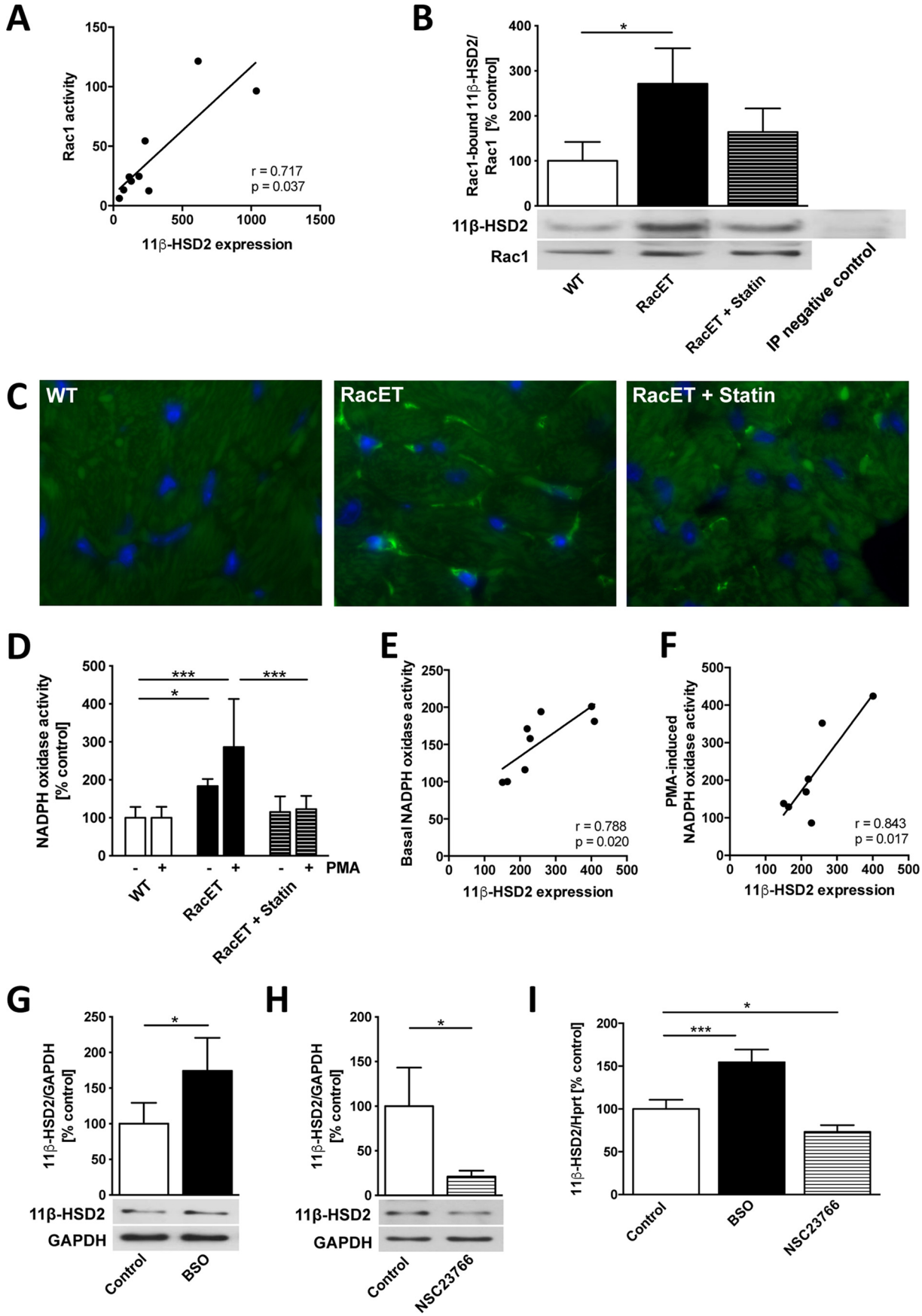
A
Rac1 activity
11β-HSD2 expression
r = 0.717
p = 0.037
B
Rac1-bound 11β-HSD2/ Rac1 [% control]
11β-HSD2
Rac1
WT
RacET
RacET + Statin
IP negative control
C
WT
RacET
RacET + Statin
D
NADPH oxidase activity [% control]
PMA
WT
RacET
RacET + Statin
E
Basal NADPH oxidase activity
11β-HSD2 expression
r = 0.788
p = 0.020
F
PMA-induced NADPH oxidase activity
11β-HSD2 expression
r = 0.843
p = 0.017
G
11β-HSD2/GAPDH [% control]
11β-HSD2
GAPDH
Control
BSO
H
11β-HSD2/GAPDH [% control]
11β-HSD2
GAPDH
Control
NSC23766
I
11β-HSD2/Hprt [% control]
Control
BSO
NSC23766

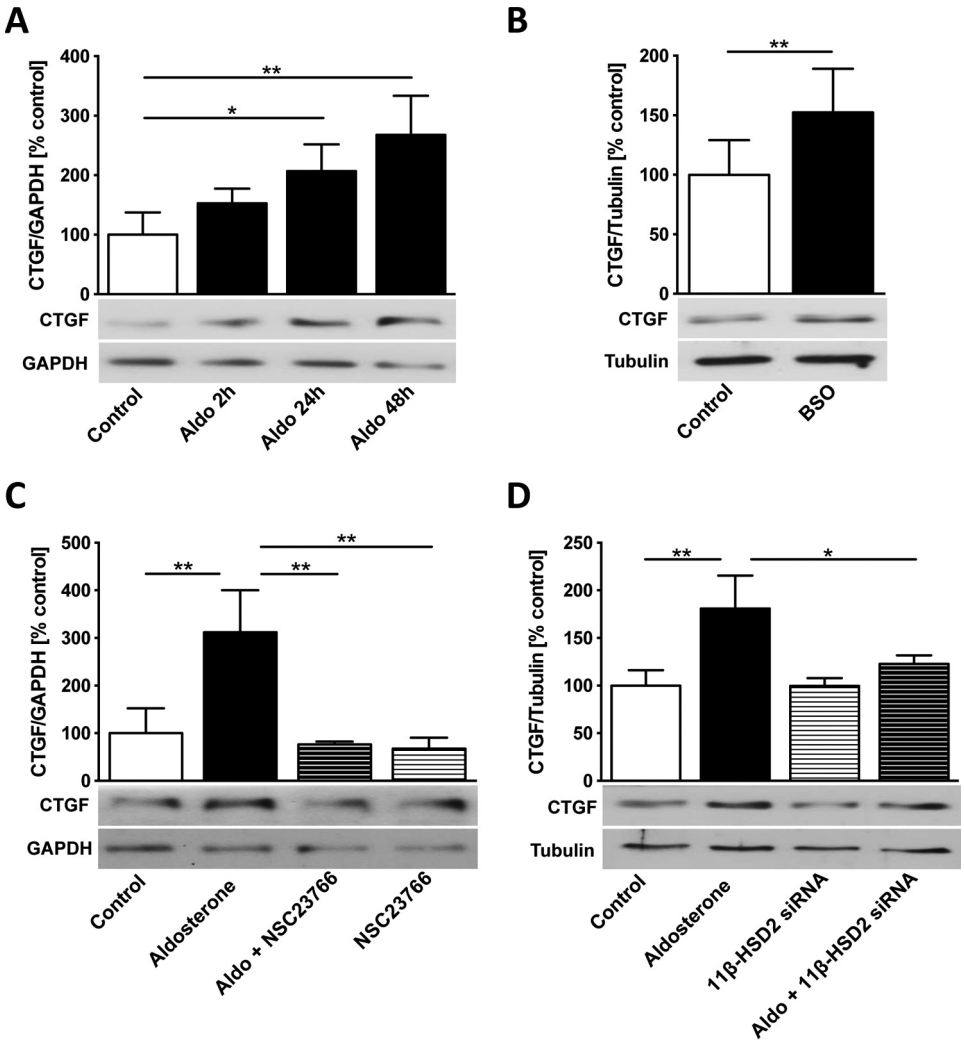

Figure 4. Rac1 and 11β-HSD2 control the aldosterone-induced CTGF up-regulation. *A*, aldosterone (*Aldo*) treatment time course (10 nM for 2 h, 24 h, and 48 h) on CTGF protein expression (Western blot) in H9c2 cardiomyocytes. *B*, connective tissue growth factor (CTGF) protein expression in L-buthionine sulfoximine (BSO)-treated (0.5 nM, 24 h) H9c2 cardiomyocytes. *C*, CTGF protein expression in cardiomyocytes treated with aldosterone (10 nM, 48 h), NSC23766 (100 μM, 48 h), or aldosterone + NSC23766 (NSC23766, 100 μM, 49 h). *D*, CTGF protein expression in H9c2 cardiomyocytes transfected with 11β-HSD2 small interfering RNA (siRNA) (7-h incubation) with or without following aldosterone treatment (10 nM, 48 h). *Error bars* indicate means ± S.D. *, $p < 0.05$; **, $p < 0.01$.

as an increased Rac1-bound 11β-HSD2 protein expression. These data indicate a direct interaction and regulation of 11β-HSD2 through Rac1. Both the 11β-HSD2 expression and the Rac1–11β-HSD2 interaction are reduced with statin treatment that inhibits the Rac1 activity in RacET mice (10). Immunostaining illustrates that the quantitative up-regulation of 11β-HSD2 expression in RacET mice is associated with a specific accumulation pattern of 11β-HSD2 in the myocardium that is reversed by statin treatment. Increased NAPDH oxidase activity closely correlates with 11β-HSD2 expression in RacET mice that suggests oxidative stress to be the mechanism by which Rac1 regulates 11β-HSD2 expression. This hypothesis is further supported by the *in vitro* data showing that BSO, a Rac1 activator generating reactive oxygen species (12), increases 11β-HSD2 expression. Additionally, 2-month-old RacET mice without any structural remodeling exhibit a similar NADPH oxidase activity and 11β-HSD2 expression compared with wild type mice, supporting the concept that oxidative stress may be required for 11β-HSD2 up-regulation by Rac1.

The enzyme 11β-HSD2 inactivates cortisol by oxidation to cortisone. Cortisol usually occupies the MR without activating the receptor because of its 100-fold higher plasma concentra-

Figure 3. Interaction of 11β-HSD2 and Rac1. *A*, correlation between Rac1 activity (assessed by pulldown assay) and 11β hydroxysteroid dehydrogenase type 2 (11β-HSD2) protein expression (Western blot) in the left atrial myocardium from patients who underwent mitral valve surgery. *B*, Rac1-bound 11β-HSD2 protein expression (immunoprecipitation) in vehicle or statin-treated RacET compared with WT mice relative to Rac1 protein expression. The *right band* represents the negative control for the immunoprecipitation (RacET left ventricular (LV) myocardium incubated with Protein A Sepharose without Rac1 antibody). *C*, 11β-HSD2 immunostaining (FITC) in WT, RacET, and RacET + statin LV myocardium, ×1000 magnification. *D*, NADPH oxidase activity with and without induction by phorbol-12-myristate13-acetate (PMA) in WT, RacET, and RacET + statin LV myocardium. *E* and *F*, correlation between 11β-HSD2 protein expression and basal (*E*) and PMA-induced (*F*) NADPH oxidase activity in RacET and RacET + statin LV myocardium. *G* and *H*, 11β-HSD2 protein expression (Western blot) in H9c2 cardiomyocytes treated with L-buthionine sulfoximine (BSO) (0.5 nM, 24 h) (*G*) and with NSC23766 (100 μM, 24h) (*H*). *I*, 11β-HSD2 mRNA expression assessed by TaqMan gene expression assay in H9c2 cardiomyocytes treated with BSO or NSC23766. *Error bars* indicate means ± S.D. *, $p < 0.05$; ***, $p < 0.001$.

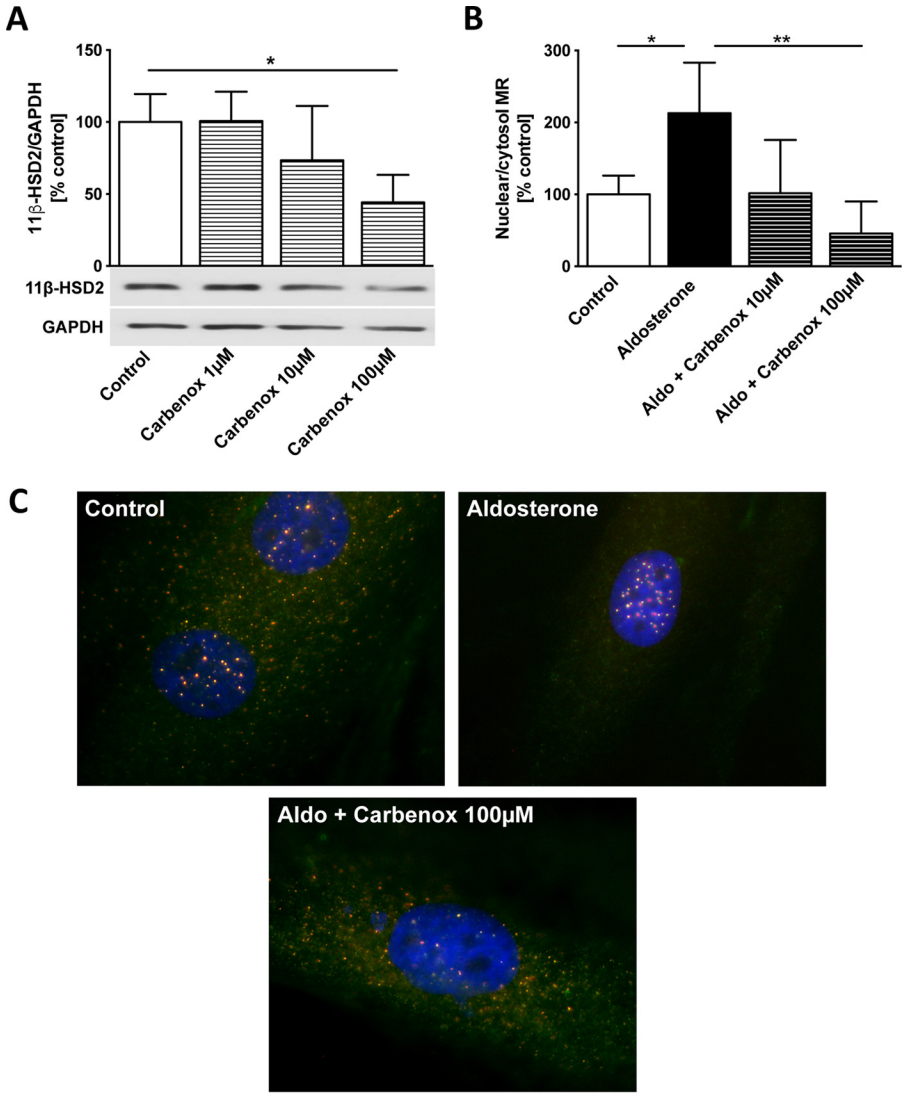

Figure 5. Inhibition of 11β-HSD2 suppressed the aldosterone-induced MR nuclear translocation. *A*, 11β hydroxysteroid dehydrogenase type 2 (11β-HSD2) protein expression (Western blot) in H9c2 cardiomyocytes treated with carbenoxolone (*Carbenox*) 1 μM, 10 μM, and 100 μM for 48 h. *B*, quantification of the nuclear translocation of the mineralocorticoid receptor (MR) in H9c2 cardiomyocytes treated with aldosterone (*Aldo*) (10 nM, 48 h) alone and in combination with carbenoxolone (10 μM and 100 μM, 49 h). mRNA polymerase II and GAPDH served as loading control for the nuclear and cytosolic fraction, respectively. *C*, representative immunohistological MR staining (FITC: Troponin; TRITC: MR; ×1000 magnification) in H9c2 cardiomyocytes treated with aldosterone (10 nM, 48 h) and both aldosterone and carbenoxolone (100 μM, 49 h). *Error bars* indicate means ± S.D. *, $p < 0.05$; **, $p < 0.01$.

tion than aldosterone. Therefore, 11β-HSD2 provides aldosterone access to the MR (14). The experiments in cultured cardiomyocytes determine the impact of 11β-HSD2 for aldosterone-induced nuclear MR translocation and for CTGF expression, *i.e.* for MR-mediated pro-fibrotic signaling. MR nuclear translocation represents activation of the receptor (15) because aldosterone induces its pro-fibrotic effects through an MR-mediated genomic pathway (16). Because *in vitro* experiments in cardiomyocytes were performed in the absence of cortisol, the results suggest that 11β-HSD2 functionally affects MR signaling independent of its cortisol-inactivating properties, *i.e.* at the receptor level or through downstream signaling. Odermatt *et al.* (15) showed that 11β-HSD2 regulates the intracellular localization of the MR and proposed a direct molecular interaction between 11β-HSD2 and MR. They provided evidence that this functional interaction of 11β-HSD2 and MR depends on a structural component of 11β-HSD2 rather than on its cortisol-metabolizing dehydrogenase function. Whether 11β-HSD2 influences MR signaling via its cortisol-inactivating enzymatic action or via a potential direct interaction with the MR is an important topic for future research.

Taken together, our data support the concept of a functional interaction between Rac1 and 11β-HSD2 that may be of importance for MR activation and subsequent pro-fibrotic signaling. We have recently shown that 11β-HSD2 is associated with atrial fibrillation and correlates with atrial fibrosis (8). This study shows for the first time that Rac1 GTPase operates as regulator of 11β-HSD2 during atrial structural remodeling that might be particularly relevant in the pathophysiology of atrial fibrillation. Oxidative stress seems to be the mediator between Rac1 and 11β-HSD2 expression.

In the literature, a relationship between 11β-HSD2 and Rac1 GTPase, either in general or during cardiac remodeling, has not been described. Several studies report functional associations

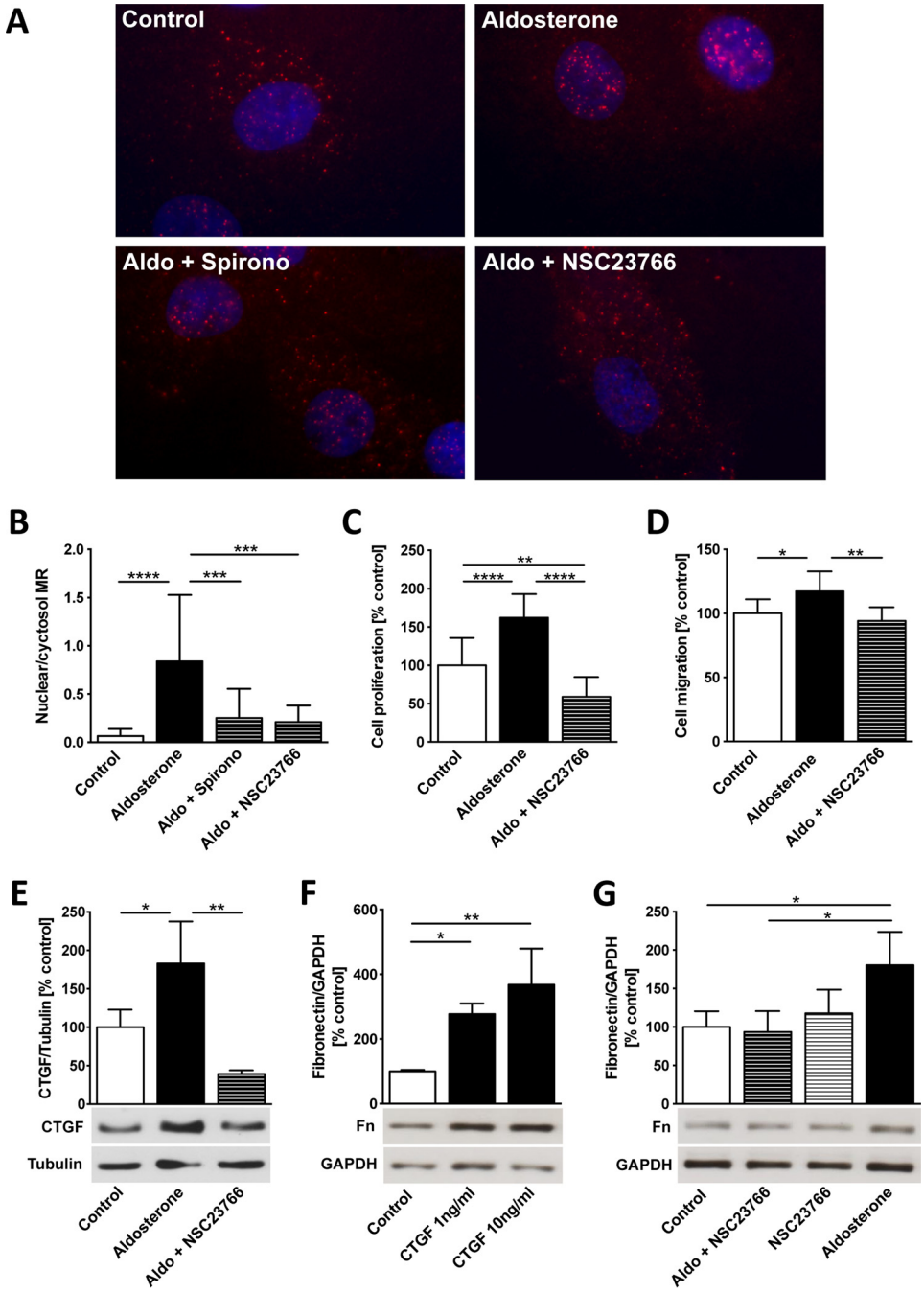

Figure 6. Rac1 regulates MR nuclear translocation, proliferation, migration, CTGF, and fibronectin in cardiac fibroblasts. *A*, neonatal rat cardiac fibroblasts were treated with aldosterone (*Aldo*) (10 nM, 24 h) with and without preincubation with spironolactone (*Spirono*) (500 nM, 25 h) and NSC23766 (100 μM, 25 h) for MR immunohistochemical staining (TRITC), ×1000 magnification. *B*, MR nuclear translocation was quantified as the ratio of nuclear to cytosolic mineralocorticoid receptor localization per cell in ×1000 magnification. *C*, fibroblast proliferation after aldosterone with and without pretreatment with NSC23766 treatment using CyQUANT assay based on DNA fluorescence. *D*, cell migration through 8.0-μm pore polyethylene terephthalate membranes in cardiac fibroblasts treated with aldosterone with and without pretreatment with NSC23766. *E*, connective tissue growth factor (CTGF) protein expression (Western blot) in cardiac fibroblasts treated with aldosterone with and without preincubation with NSC23766. *F*, fibronectin protein expression (Western blot) in cardiac fibroblasts treated with CTGF (1 ng/ml and 10 ng/ml for 1 h). *G*, fibronectin protein expression in aldosterone-treated cardiac fibroblasts with and without NSC23766 pretreatment assessed by Western blotting. *Error bars* indicate means ± S.D. *, $p < 0.05$; **, $p < 0.01$; ***, $p < 0.001$; ****, $p < 0.0001$.

between the Rac1 GTPase and MR signaling during renal and cardiac pathology. The Rac1-MR pathway contributes to salt-sensitive hypertension (17, 18) and renal injury (18, 19). In cardiomyocytes, Nagase *et al.* (12) showed that Rac1 modulates MR transcriptional activity through oxidative stress. Recently, Ayuzawa *et al.* (20) described Rac1-mediated MR activation in an animal model of pressure overload leading to cardiac hypertrophy. Kimura *et al.* (21) studied atrial fibrosis and atrial fibrillation inducibility in hypertensive rats, which were prevented by the MR antagonist eplerenone. Despite this evidence of interaction, the precise mechanisms by which Rac1 influences MR signaling remain unknown. Specifically, these studies did not address the impact of the Rac1-MR pathway for the development of cardiac fibrosis. Our data show that Rac1 regulates

11β-HSD2 in the myocardium, which is associated with downstream fibrotic remodeling.

This is a mechanistic study evaluating the role of Rac1 for MR pro-fibrotic signaling at the cellular level. We used CTGF as a marker of fibrosis because CTGF is a well established pro-fibrotic mediator that is expressed by both cardiomyocytes and cardiac fibroblasts (8, 9, 22). Furthermore, aldosterone induces cardiac fibroblast proliferation, migration, and fibronectin expression via a Rac1 GTPase-dependent pathway. These data demonstrate the importance of Rac1 for fibrotic remodeling. However, there are no specific pharmacological inhibitors of Rac1 available for systemic application. Statins were observed to down-regulate the activity of small G proteins, *i.e.* Rac1, in the myocardium (11). In a previous study, statins did not reduce the amount of fibrosis in RacET mice (10).

Clinically, perioperative administration of statins failed to reduce the incidence of postoperative atrial fibrillation in patients undergoing cardiac surgery (23). In contrast, MR antagonists have been shown to prevent cardiac fibrosis at molecular and organ level (6, 8). In the randomized trial of spironolactone in congestive heart failure (RALES) high levels of circulating biomarkers of myocardial fibrosis were associated with poor outcome. Spironolactone treatment reduced the level of circulating biomarkers of fibrosis (24). Eplerenone reduced the incidence of atrial fibrillation in patients with systolic heart failure and mild symptoms (EMPHASIS-HF trial) (25). Whether a specific Rac1 inhibition could have any additional or synergistic effect on MR antagonists for prevention of cardiac fibrosis or atrial fibrillation remains to be investigated.

Conclusion

This study demonstrates a new role of Rac1 regulating 11β-HSD2. Rac1 promotes aldosterone-induced MR activation and downstream pro-fibrotic pathways through CTGF. Rac1 may be a therapeutic target to inhibit MR signaling and prevent structural cardiac remodeling.

Experimental procedures

Transgenic RacET mice

Mice with cardiac overexpression of constitutively active Rac1 under the control of the α-myosin heavy chain promoter (RacET) (26) and wild type control mice (FVBN) were fed with normal or rosuvastatin-supplemented (0.4 mg/day) chow over 10 months as reported recently (10). Heart rate, regularity, and presence of P waves were documented by 6-channel electrocardiography recording at 6 and 12 months of age. The study was approved by the Ethical Review Board of the Universität des Saarlandes and is in accord with the "Guide for the Care and Use of Laboratory Animals" published by the National Institutes of Health (NIH Pub. No. 85-23, revised 1996).

Human left atrial tissue

Myocardial tissue samples of the left atrial appendage were derived from patients who underwent mitral valve cardiac surgery (8, 10). The patients did not receive drugs at least 12 h before surgery. The analysis was approved by the Ethical Review Board of the Ärztekammer des Saarlandes (No.131/00). Rac1 activity was assessed using Rac1 GST-p21-activated kinase pulldown assay as described (10).

Cell isolation and culture

Cardiac fibroblasts were isolated from 3- to 5-day-old neonatal Sprague-Dawley rat hearts (Charles River Laboratories, Köln, Germany) of mixed sex as described (8, 9). Fibroblasts were separated by adhesion from cardiomyocytes and the purity of the fibroblasts was confirmed by vimentin staining. Fibroblasts were used until passage three to prevent differentiation. H9c2 cardiomyocytes (LGC Promochem, Wesel, Germany) are an immortalized cell line derived from rat cardiac tissue (27). Experiments were performed at passage 18–23. Cardiac fibroblasts were grown in Dulbecco's modified Eagle's medium (DMEM) and cardiomyocytes were grown in F-10 nutrition mixture (Invitrogen), both supplemented with 10% (v/v) fetal calf serum, gentamicin (0.08 mg/ml), and penicillin (100 IU/ml) and maintained in 95% air and 5% CO_2 at 37 °C. When subconfluent, cells were kept in serum-free medium for 24 h before treatment.

Specification of drugs

Aldosterone (Sigma-Aldrich) is a physiological mineralocorticoid, which induces cardiac fibrosis via binding at the mineralocorticoid receptor (MR) (8). Spironolactone (Sigma-Aldrich) is a commercially available MR antagonist. Rosuvastatin possesses the property to down-regulate the activity of small G proteins, *i.e.* Rac1, in the myocardium (11). L-buthionine sulfoximine (BSO), a selective inhibitor of γ-glutamylcysteine synthetase, is a Rac1 activator through oxidative stress via glutathione depletion (12). NSC23766 (Sigma-Aldrich) is a Rac-specific small-molecule inhibitor (9, 28). Carbenoxolone (Sigma-Aldrich) is an active metabolite from glycyrrhizic acid and an inhibitor of 11β-HSD2 (13). Connective tissue growth factor (CTGF) is a central pro-fibrotic mediator during cardiac remodeling established in previous studies (8, 9, 29).

Small interfering ribonucleic acid (siRNA) transfection

Transfection of H9c2 cardiomyocytes with CTGF small interfering 11β-HSD2 RNA (sc-270598, Santa Cruz Technology) was performed according to the manufacturer's instructions. When 60–80% confluent, cells were incubated with 80 pM 11β-HSD2 siRNA for 7 h. After growing in DMEM for 24 h, cells were treated and harvested as described above. Fluorescein-conjugated scrambled siRNA (sc-36869, Santa Cruz) was used as negative control for transfection.

Western blotting analysis

Total protein lysates were prepared as described (11). Cellular protein content was quantified by a modified Lowry assay. Immunoblotting was performed using anti-MR (rabbit polyclonal antibody against amino acids 1–300 of MR of human origin) (sc-11412, Santa Cruz), anti-11β-HSD2 (mouse monoclonal antibody against amino acids 261–405 of 11β-HSD2 of human origin) (sc-365529, Santa Cruz), anti-CTGF (goat polyclonal antibody against a peptide mapping within an internal region of CTGF of human origin) (sc-14939, Santa Cruz), anti-Sprouty-1 (rabbit polyclonal antibody against amino acids

61–180 mapping within an internal region of Sprouty-1 of human origin) (sc-30048, Santa Cruz), anti-LOX (rabbit polyclonal antibody against residues 350 to the C terminus of human LOX) (ab31238, Abcam), anti-Rac1 (mouse IgG_{2b} against recombinant protein containing the full-length human Rac1, Clone 23A8) (05–389, EMD Millipore) and anti-fibronectin (mouse monoclonal antibody against a T cell leukemia biopsy of human origin) (sc-71113, Santa Cruz). Anti-tubulin (rabbit polyclonal antibody against amino acids 210–444 of β-tubulin of human origin) (sc-9104, Santa Cruz) and anti-GAPDH (mouse monoclonal antibody against GAPDH purified from muscle of rabbit origin) (sc-32233, Santa Cruz) were used for protein loading control. Immunodetection was accomplished using goat anti-rabbit, goat anti-mouse, or rabbit anti-goat secondary antibody (1:4000 dilution) (Sigma) and an enhanced chemiluminescence kit (Amersham Biosciences) followed by densitometry.

Fibroblast proliferation and migration

Fibroblast proliferation was analyzed by CyQUANT® assay according to the manufacturer's protocol (Invitrogen) as described recently (30). Briefly, cardiac fibroblasts in passage two or three were plated at 500, 1000, and 2000 cells per well into 96-well clear-bottom plates (BD Biosciences) and allowed to attach overnight. After 24 h, the cells were fed with serum-free medium for 24 h followed by treatment with aldosterone (10 μM) and NSC23766 (100 μM) as indicated. After removing the medium, the plates were frozen at −80 °C for 24 h before assay. Thawed plates were stained with CyQUANT® GR dye and fluorescence quantified on a microplate fluorescence reader (Tecan Group Ltd., Männedorf, Switzerland) using 480 excitation and 520 emission filters. Fibroblast proliferation quantification was adjusted to vehicle-treated control for each cell count.

Cardiac fibroblast migration was quantified using FluoroBlok cell culture inserts (BD Biosciences) and 8.0-μm pore polyethylene terephthalate membranes. Briefly, cardiac fibroblasts were trypsinized and suspended in DMEM. 1 ml of medium containing 2.0×10^5 cells was layered on the insert membranes. Fibroblasts were treated with aldosterone (10 nM) and NSC237656 (100 μM). The lower chamber contained medium with 10% serum. The cells were incubated for 24 h at 37 °C. Afterward, the membranes were washed with PBS, the lower membrane surfaces were stained with DAPI, and the number of invaded cells quantified.

NADPH oxidase activity assay

NADPH oxidase activity was measured by a lucigenin-enhanced chemiluminescence assay in buffer B containing (in mmol/liter) phosphate 50, pH 7.0, EGTA 1, protease inhibitors (cOmplete®, Roche), sucrose 150, lucigenin 0.005, and NADPH 0.1 as described (31). Tissue was mechanically lysed using a Teflon homogenizer in ice-cold buffer B, lacking lucigenin and substrate. Lysates of left ventricular myocardium were incubated in the presence or absence of PMA, 1 μmol/liter, 10 min, 37 °C. 250-μl aliquots of the protein sample were measured using NADPH as substrate in a scintillation counter (Berthold Lumat LB 9507) in 1-min intervals. Total protein concentration was adjusted to 1 mg/ml.

Immunoprecipitation analysis

Protein A Sepharose CL-4B beads (GE Healthcare) were solved in immunoprecipitation buffer (50 mM Tris-HCl, 150 mM NaCl, 2 mM MgCl, 10% glycerol, 1% IGEPAL, phosphatase inhibitors, protease inhibitors, 1 mM PMSF) and incubated with Rac1 antibody (clone 23A8, Upstate Biotechnology, Waltham, MA) overnight at 4 °C. WT and RacET myocardium were homogenized in immunoprecipitation buffer, centrifuged, and the supernatant used for further analysis. After protein content quantification by a modified Lowry assay, 1 mg of myocardial protein was added to the Sepharose beads-Rac1 antibody conjunction in immunoprecipitation buffer and incubated overnight at 4 °C. Sepharose beads without Rac1 served as negative control. After centrifugation, the pellet was washed with immunoprecipitation buffer and the protein content of Rac1-bound 11β-HSD2 quantified by Western blotting.

RT-PCR and TaqMan gene expression assay

Total RNA isolation, reverse transcription, and competitive PCR were performed according to standard techniques. The following primers were used: rat CTGF forward 5′-AGAGTGGAGATGCCAGGAGA-3′; rat CTGF reverse 5′-CACACACCCAGCTCTTGCTA-3′; rat GAPDH forward 5′-AGACAGCCGCATCTTCTTGT-3′; rat GAPDH reverse 5′-CTTGCCGTGGGTAGAGTCAT-3′. GAPDH was amplified as external standard. Each PCR cycle consisted of denaturing at 95 °C for 45 s, annealing at 55 °C and 63 °C for 30 s for rat CTGF and GAPDH, respectively, and elongation at 72 °C for 60 s. Equal amounts of corresponding target gene and GAPDH RT-PCR products were loaded on 1.5% agarose gels and optical densities of ethidium bromide-stained DNA bands were quantified.

11β-HSD2 gene expression was analyzed using TaqMan gene expression assay (Applied Biosystems) with Assay ID Mm01251104_01 and Rn00492539_m1. Hrpt1 served as housekeeping gene (Assay ID Rn01527840_m1).

Histological and immunofluorescence staining

Cryosections (10 μm) were stained with 0.1% Sirius Red F3BA (Polysciences Inc.) as described (10). Immunofluorescence was performed on cultured H9c2 cardiomyocytes and neonatal cardiac fibroblasts applying anti-MR antibody (sc-11412, Santa Cruz) and anti-troponin antibody (sc-8123, Santa Cruz) in H9c2 cardiomyocytes. Paraffin-embedded RacET and wild type mice myocardium were stained with anti-11β-HSD2 antibody (sc-365529, Santa Cruz). Fluorescein isothiocyanate (FITC)- or tetramethylrhodamine isothiocyanate (TRITC)-conjugated anti-rabbit, anti-mouse, or anti-goat IgG (dianova GmbH, Hamburg, Germany) were used as secondary antibodies. Sections were counterstained with DAPI (Calbiochem, Darmstadt, Germany). A negative control for nonspecific staining was performed in a parallel section. MR translocation was quantified as the ratio nuclear to cytoplasm MR localization for $n = 14$ cells per group in one layer. The analyzer was blinded about the pharmacological treatment of the cells.

Nuclear MR fraction extraction

Treated H9c2 cells were harvested in cytosolic lysis buffer (10 nM HEPES, 10 nM KCl, 0.1 mM EDTA, 0.1 mM EGTA, 1 nM DTT, 0.5 mM PMSF, protease inhibitors (cOmplete)). After 15 min of swelling, 10% Nonidet P-40 was added, vortexed over 10 min, and centrifuged. The supernatant represented the cytosolic protein fraction. The nuclear pellet was resuspended in nuclear lysis buffer (20 nM HEPES, 0.4 M NaCl, 1 mM EDTA, 1 mM EGTA, 1 nM DTT, 0.5 mM PMSF, protease inhibitors (cOmplete)), mechanically lysed during 15 min, and centrifuged with the supernatant representing the nuclear proteins. Both the cytosolic and the nuclear fraction were further analyzed by Western blotting with MR antibodies.

Statistical analysis

Band intensities were analyzed by densitometry. Data were calculated from at least three independent experiments and are presented as mean and standard deviation. Statistical analyses were calculated using GraphPad Prism 6. We performed unpaired Student's *t* test for single comparison and analysis of variance (ANOVA) followed by Newman-Keuls post hoc analysis for multiple comparisons, respectively. Differences were considered significant at $p < 0.05$.

Author contributions—D. L. substantially contributed to conception and design and acquisition, analysis, and interpretation of the data; drafted the article; and approved the final version to be published. P. S. substantially contributed to acquisition, analysis, and interpretation of data and approved the final version to be published. N. J. substantially contributed to acquisition, analysis, and interpretation of data and approved the final version to be published. A. K. substantially contributed to acquisition, analysis, and interpretation of data and approved the final version to be published. M. B. revised the article critically for important intellectual content and approved the final version to be published. U. L. substantially contributed to conception, design, and interpretation of data; revised the article critically for important intellectual content; and approved the final version to be published.

Acknowledgments—We thank Simone Jäger and Ellen Becker for their excellent technical assistance.

References

1. Travers, J. G., Kamal, F. A., Robbins, J., Yutzey, K. E., and Blaxall, B. C. (2016) Cardiac fibrosis: the fibroblast awakens. *Circ. Res.* **118,** 1021–1040
2. Rockey, D. C., Bell, P. D., and Hill, J. A. (2015) Fibrosis—a common pathway to organ injury and failure. *N. Engl. J. Med.* **372,** 1138–1149
3. Dzeshka, M. S., Lip, G. Y., Snezhitskiy, V., and Shantsila, E. (2015) Cardiac fibrosis in patients with atrial fibrillation: mechanisms and clinical implications. *J. Am. Coll. Cardiol.* **66,** 943–959
4. Lip, G. Y., Tse, H. F., and Lane, D. A. (2012) Atrial fibrillation. *Lancet* **379,** 648–661
5. Young, M. J. (2008) Mechanisms of mineralocorticoid receptor-mediated cardiac fibrosis and vascular inflammation. *Curr. Opin. Nephrol. Hypertens.* **17,** 174–180
6. Bauersachs, J., Jaisser, F., and Toto, R. (2015) Mineralocorticoid receptor activation and mineralocorticoid receptor antagonist treatment in cardiac and renal diseases. *Hypertension* **65,** 257–263
7. Ponikowski, P., Voors, A. A., Anker, S. D., Bueno, H., Cleland, J. G., Coats, A. J., Falk, V., González-Juanatey, J. R., Harjola, V. P., Jankowska, E. A., Jessup, M., Linde, C., Nihoyannopoulos, P., Parissis, J. T., Pieske, B., *et al.* (2016) 2016 ESC Guidelines for the diagnosis and treatment of acute and chronic heart failure: The Task Force for the diagnosis and treatment of acute and chronic heart failure of the European Society of Cardiology (ESC). *Eur. Heart J.* **37,** 2129–2200
8. Lavall, D., Selzer, C., Schuster, P., Lenski, M., Adam, O., Schäfers, H. J., Böhm, M., and Laufs, U. (2014) The mineralocorticoid receptor promotes fibrotic remodeling in atrial fibrillation. *J. Biol. Chem.* **289,** 6656–6668
9. Adam, O., Lavall, D., Theobald, K., Hohl, M., Grube, M., Ameling, S., Sussman, M. A., Rosenkranz, S., Kroemer, H. K., Schäfers, H. J., Böhm, M., and Laufs, U. (2010) Rac1-induced connective tissue growth factor regulates connexin 43 and N-cadherin expression in atrial fibrillation. *J. Am. Coll. Cardiol.* **55,** 469–480
10. Adam, O., Frost, G., Custodis, F., Sussman, M. A., Schäfers, H. J., Böhm, M., and Laufs, U. (2007) Role of Rac1 GTPase activation in atrial fibrillation. *J. Am. Coll. Cardiol.* **50,** 359–367
11. Laufs, U., Kilter, H., Konkol, C., Wassmann, S., Böhm, M., and Nickenig, G. (2002) Impact of HMG CoA reductase inhibition on small GTPases in the heart. *Cardiovasc. Res.* **53,** 911–920
12. Nagase, M., Ayuzawa, N., Kawarazaki, W., Ishizawa, K., Ueda, K., Yoshida, S., and Fujita, T. (2012) Oxidative stress causes mineralocorticoid receptor activation in rat cardiomyocytes: role of small GTPase Rac1. *Hypertension* **59,** 500–506
13. Duax, W. L., Ghosh, D., and Pletnev, V. (2000) Steroid dehydrogenase structures, mechanism of action, and disease. *Vitam. Horm.* **58,** 121–148
14. Odermatt, A., and Kratschmar, D. V. (2012) Tissue-specific modulation of mineralocorticoid receptor function by 11β-hydroxysteroid dehydrogenases: an overview. *Mol. Cell. Endocrinol.* **350,** 168–186
15. Odermatt, A., Arnold, P., and Frey, F. J. (2001) The intracellular localization of the mineralocorticoid receptor is regulated by 11β-hydroxysteroid dehydrogenase type 2. *J. Biol. Chem.* **276,** 28484–28492
16. Funder, J. W. (2006) Minireview. Aldosterone and the cardiovascular system: genomic and nongenomic effects. *Endocrinology* **147,** 5564–5567
17. Shibata, S., Mu, S., Kawarazaki, H., Muraoka, K., Ishizawa, K., Yoshida, S., Kawarazaki, W., Takeuchi, M., Ayuzawa, N., Miyoshi, J., Takai, Y., Ishikawa, A., Shimosawa, T., Ando, K., Nagase, M., and Fujita, T. (2011) Rac1 GTPase in rodent kidneys is essential for salt-sensitive hypertension via a mineralocorticoid receptor-dependent pathway. *J. Clin. Invest.* **121,** 3233–3243
18. Kawarazaki, H., Ando, K., Shibata, S., Muraoka, K., Fujita, M., Kawarasaki, C., and Fujita, T. (2012) Mineralocorticoid receptor–Rac1 activation and oxidative stress play major roles in salt-induced hypertension and kidney injury in prepubertal rats. *J. Hypertens.* **30,** 1977–1985
19. Shibata, S., Nagase, M., Yoshida, S., Kawarazaki, W., Kurihara, H., Tanaka, H., Miyoshi, J., Takai, Y., and Fujita, T. (2008) Modification of mineralocorticoid receptor function by Rac1 GTPase: implication in proteinuric kidney disease. *Nat. Med.* **14,** 1370–1376
20. Ayuzawa, N., Nagase, M., Ueda, K., Nishimoto, M., Kawarazaki, W., Marumo, T., Aiba, A., Sakurai, T., Shindo, T., and Fujita, T. (2016) Rac1-Mediated Activation of Mineralocorticoid Receptor in Pressure Overload-Induced Cardiac Injury. *Hypertension* **67,** 99–106
21. Kimura, S., Ito, M., Tomita, M., Hoyano, M., Obata, H., Ding, L., Chinushi, M., Hanawa, H., Kodama, M., and Aizawa, Y. (2011) Role of mineralocorticoid receptor on atrial structural remodeling and inducibility of atrial fibrillation in hypertensive rats. *Hypertens. Res.* **34,** 584–591
22. Koitabashi, N., Arai, M., Kogure, S., Niwano, K., Watanabe, A., Aoki, Y., Maeno, T., Nishida, T., Kubota, S., Takigawa, M., and Kurabayashi, M. (2007) Increased connective tissue growth factor relative to brain natriuretic peptide as a determinant of myocardial fibrosis. *Hypertension* **49,** 1120–1127
23. Zheng, Z., Jayaram, R., Jiang, L., Emberson, J., Zhao, Y., Li, Q., Du, J., Guarguagli, S., Hill, M., Chen, Z., Collins, R., and Casadei, B. (2016) Perioperative rosuvastatin in cardiac surgery. *N. Engl. J. Med.* **374,** 1744–1753
24. Zannad, F., Alla, F., Dousset, B., Perez, A., and Pitt, B. (2000) Limitation of excessive extracellular matrix turnover may contribute to survival benefit of spironolactone therapy in patients with congestive heart failure. Insights from the Randomized Aldactone Evaluation Study (RALES). *Circulation* **102,** 2700–2706
25. Swedberg, K., Zannad, F., McMurray, J. J., Krum, H., van Veldhuisen, D. J., Shi, H., Vincent, J., and Pitt, B. (2012) Eplerenone and atrial fibrillation in mild systolic heart failure. Results from the EMPHASIS-HF (Eplerenone

in Mild Patients Hospitalization And SurvIval Study in Heart Failure) Study. *J. Am. Coll. Cardiol.* **59,** 1598–1603
26. Sussman, M. A., Welch, S., Walker, A., Klevitsky, R., Hewett, T. E., Price, R. L., Schaefer, E., and Yager, K. (2000) Altered focal adhesion regulation correlates with cardiomyopathy in mice expressing constitutively active rac1. *J. Clin. Invest.* **105,** 875–886
27. Hescheler, J., Meyer, R., Plant, S., Krautwurst, D., Rosenthal, W., and Schultz, G. (1991) Morphological, biochemical, and electrophysiological characterization of a clonal cell (H9c2) line from rat heart. *Circ. Res.* **69,** 1476–1486
28. Gao, Y., Dickerson, J. B., Guo, F., Zheng, J., and Zheng, Y. (2004) Rational design and characterization of a Rac GTPase-specific small molecule inhibitor. *Proc. Natl. Acad. Sci. U.S.A.* **101,** 7618–7623
29. Adam, O., Theobald, K., Lavall, D., Grube, M., Kroemer, H. K., Ameling, S., Schäfers, H. J., Böhm, M., and Laufs, U. (2011) Increased lysyl oxidase expression and collagen cross-linking during atrial fibrillation. *J. Mol. Cell. Cardiol.* **50,** 678–685
30. Mummidi, S., Das, N. A., Carpenter, A. J., Kandikattu, H., Krenz, M., Siebenlist, U., Valente, A. J., and Chandrasekar, B. (2016) Metformin inhibits aldosterone-induced cardiac fibroblast activation, migration and proliferation *in vitro*, and reverses aldosterone + salt-induced cardiac fibrosis *in vivo*. *J. Mol. Cell. Cardiol.* **98,** 95–102
31. Custodis, F., Eberl, M., Kilter, H., Böhm, M., and Laufs, U. (2006) Association of RhoGDIα with Rac1 GTPase mediates free radical production during myocardial hypertrophy. *Cardiovasc. Res.* **71,** 342–351